UC Berkeley
UC Berkeley Previously Published Works

Title

Cryptotriton Phylogeny and Biogeography

Permalink

Journal

ISSN

Authors

Rovito, Sean M
Vásquez-Almazán, Carlos R
Papenfuss, Theodore J
et al.

Publication Date

DOI

Biogeography and evolution of Central American cloud forest salamanders (Caudata: Plethodontidae: *Cryptotriton*), with the description of a new species

SEAN M. ROVITO[1,2]*, CARLOS R. VÁSQUEZ-ALMAZÁN[3], THEODORE J. PAPENFUSS[1], GABRIELA PARRA-OLEA[2] and DAVID B. WAKE[1]

[1]*Museum of Vertebrate Zoology, University of California, 3101 Valley Life Sciences Building, Berkeley, CA 94720-3160, USA*
[2]*Instituto de Biología, Universidad Nacional Autónoma de México, AP 70-153, Circuito Exterior s/n, Ciudad Universitaria, México, D.F., México*
[3]*Museo de Historia Natural, Escuela de Biología, Universidad de San Carlos, Calle Mariscal Cruz 1-56, Zona 10, Ciudad de Guatemala, Guatemala*

The cloud forests of Mesoamerica are notable for their high endemism, and plethodontid salamanders provide a striking example of divergence and microendemism across cloud forest blocks at a regional level. Salamanders that make use of arboreal bromeliad microhabitats in the cloud forest appear to be especially prone to divergence driven by natural habitat fragmentation, and are expected to show high endemism at small spatial scales. We use a multilocus dataset to investigate the biogeographic history and relationships among species of a small genus of salamander, *Cryptotriton*, restricted to the cloud forests of Nuclear Central America. We use a morphological data set along with a coalescent species delimitation method to reveal the presence of at least one undescribed species from an isolated cloud forest in eastern Guatemala. Biogeographic analyses show that *Cryptotriton* has a different biogeographic history than another clade of cloud forest-restricted salamanders in the same region, perhaps indicating that each genus restricted the spatial expansion and diversification of the other through preemptive occupancy. Our results suggest that isolation across relatively short geographic distances has led to range fragmentation and deep divergence between species. Exploration of remaining patches of cloud forest likely will continue to reveal undetected diversity.

INTRODUCTION

Cloud forests worldwide are notable for the high levels of endemism of both plants and animals (Gentry, 1992; Hamilton, Juvik & Scatena, 1995). While the species richness of many groups is lower in the cloud forest than in lowland rainforests, the patchy spatial distribution of this vegetation type results in many species that are narrowly endemic at the regional or local level. Cloud forests vegetation depends on high levels of fog water (Stadtmüller, 1987; Bruijnzeel, 2001), restricting it to limited areas where elevation and climatic characteristics are appropriate for cloud formation. In Mesoamerica, cloud forests have an archipelago-like distribution (Myers, 1969; Luna-Vega *et al.*, 1999), with intervening areas of lowland habitat. Phylogeographic data from the region indicate that the history of natural

*Corresponding author. Current address: Laboratorio Nacional de Genómica para la Biodiversidad, km 9.6 Libramiento Norte Carretera León, 36821 Irapuato, Guanajuato, México. E-mail: smrovito@gmail.com

cloud forest fragmentation has had complex effects on the biota that inhabit it, with vicariant events across a single barrier occurring at different times (Ornelas *et al.*, 2013). Long-term isolation in cloud forests has led to high levels of genetic diversity within species as a result of divergence between populations in different cloud forest blocks (Daza, Castoe & Parkinson, 2010; Ornelas, Ruiz-Sánchez & Sosa, 2010; Jadin *et al.*, 2012).

Few groups exemplify the pattern of high cloud forest endemism more than the neotropical salamanders of the family Plethodontidae, which have diversified to include a large number of cloud forest specialists (Wake, 1987). Many of these species have adapted to live in cloud forest environments by specializing in the use of either arboreal bromeliads or moss mats. These environments provide moist, thermally buffered refugia (Feder, 1982), which are especially important during the dry season. The close association between these arboreal salamanders and cloud forest vegetation makes them an interesting system in which to study the impact of cloud forest fragmentation on species divergence.

Plethodontid salamander species have a relatively long history in the Neotropics (Wake & Lynch, 1976), especially in Nuclear Central America, the region between the Isthmus of Tehuantepec in southeastern Mexico and the Nicaragua Depression (Schuchert, 1935). Nuclear Central America contains multiple endemic genera, several of which are restricted to cloud forest environments, indicating the importance of the region in Neotropical plethodontid diversification. Salamanders adapted to arboreal life in the cloud forest come in various forms. Some are relatively large and long-limbed with nearly unwebbed digits (*Nyctanolis, Ixalotriton*, a few *Pseudoeurycea*). Others are medium sized to small with moderately to fully webbed digits (*Bolitoglossa*). Finally, many species are small to diminutive, and slender with slightly webbed to syndactylous digits and long, prehensile tails. This third group includes a few species of *Thorius* and a large number of species generally similar in appearance that were once contained within the genus *Chiropterotriton*. This genus formerly ranged from northern Mexico to Costa Rica, but was subsequently divided into multiple genera (Wake & Elias, 1983; García-París & Wake, 2000), and phylogenetic analyses of these small arboreal salamanders showed that they do not form a monophyletic group (García-París & Wake, 2000; Wiens *et al.*, 2007). *Chiropterotriton*, as currently recognized, occurs exclusively to the west of the Isthmus of Tehuantepec and is not closely related to species it formerly contained that are now allocated to other genera (*Cryptotriton, Dendrotriton*, and *Nototriton*). Molecular studies using both allozymes (Good & Wake, 1993; Darda, 1994; Vásquez-Almazán *et al.*, 2009) and DNA sequence data (García-París & Wake, 2000;

Parra-Olea, 2003; Townsend *et al.*, 2011; Rovito *et al.*, 2012) have shed light on relationships within and between genera and supported the recognition of many new species.

While studies of most of these genera have included nearly complete taxonomic sampling, *Cryptotriton* has been underrepresented because few specimens and tissues are available in museum collections for most species. The phylogeny of García-París & Wake (2000) included only three species of *Cryptotriton*, one of which was undescribed at the time, and a recent phylogeny (McCranie & Rovito, 2014) included only mitochondrial DNA. McCranie & Rovito (2014) did not recover strong support for interspecific relationships within *Cryptotriton*, and suggested that either more loci or the inclusion of additional, unsampled populations might help to resolve the phylogeny. Phylogenetic analysis of a similar cloud forest-restricted clade, *Dendrotriton*, showed that species formed primarily in allopatry in geologically ancient areas of Nuclear Central America, illustrating the importance of the ancient highlands of the region in generating species diversity (Rovito *et al.*, 2012). Here, we estimate a phylogeny for *Cryptotriton* based on portions of two mitochondrial and four nuclear genes. We use our phylogenetic hypothesis together with a coalescent species delimitation method and morphological data to test the hypothesis that our sample includes additional, undescribed species, and use our phylogeny and updated taxonomy to investigate the biogeographic history of *Cryptotriton* in Nuclear Central America.

METHODS

STUDY SYSTEM

Cryptotriton currently includes six species (AmphibiaWeb, 2014), all of which are found in the mountains of Nuclear Central America. *Cryptotriton alvarezdeltoroi* (Papenfuss and Wake, 1987) is known from three sites in northern Chiapas. *Cryptotriton sierraminensis* Vásquez-Almazán, Rovito, Good, and Wake, 2009 and *C. veraepacis* (Lynch & Wake, 1978) are found in the mountains of the Motagua-Polochic fault zone of eastern Guatemala. *Cryptotriton monzoni* (Campbell & Smith, 1998) is found in a small area of eastern Guatemala south of the Motagua fault. *Cryptotriton nasalis* (Dunn, 1924) and *Cryptotriton necopinus* McCranie and Rovito, 2014 are both found in the mountains of Honduras. All species of *Cryptotriton* are restricted to the cloud forest and all but *C. alvarezdeltoroi* have been found in arboreal bromeliads. *Cryptotriton monzoni* was first collected in a bromeliad (Campbell & Smith, 1998) but all recently collected specimens were found climbing on tree trunks (S. M. Rovito & C. R. Vásquez-Almazán, pers.
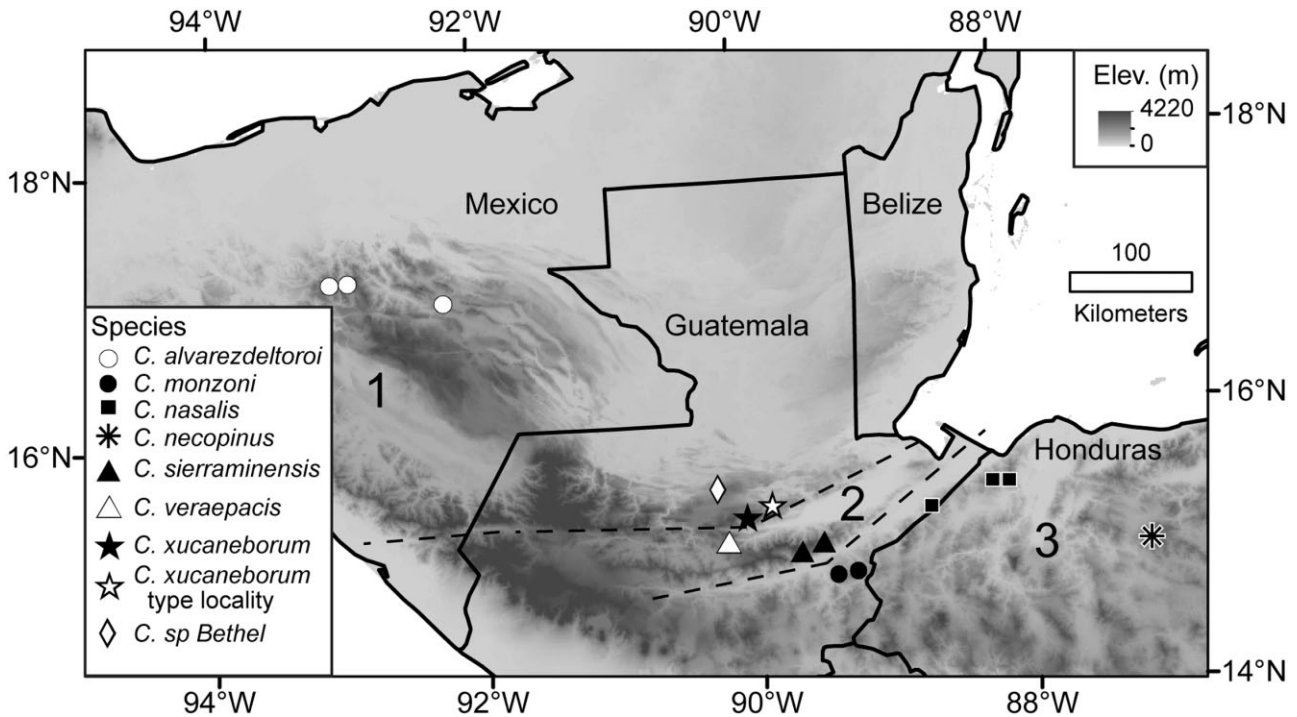
Figure 1. Map of Nuclear Central America showing the distributions of described species of *Cryptotriton*, as well as several undescribed populations from Alta Verapaz. Dotted lines separate the three geological regions used in biogeographic analysis: (1) Chiapas highlands of the Maya block, (2) Motagua-Polochic fault zone, and (3) Chortís highlands.

obs.). All species have restricted ranges (Fig. 1), and no species is known from more than three localities. Two other species were formerly assigned to *Cryptotriton*: *Cryptotriton adelos* (Papenfuss and Wake, 1987), the only species of *Cryptotriton* found west of the Isthmus of Tehuantepec, was transferred to the genus *Thorius* by Wake *et al.* (2012) on the basis of osteological and molecular evidence, and *Cryptotriton wakei* (Campbell & Smith, 1998) was synonymized with *C. nasalis* on morphological grounds (McCranie & Rovito, 2014).

DNA SEQUENCING

We collected specimens of all named species of *Cryptotriton* during multiple trips to Guatemala, Mexico, and Honduras from 2006–2013. Voucher specimens were fixed in 10% buffered formalin and stored in 70% ethanol. Liver or tail-tip tissue samples were collected in the field and either flash-frozen in liquid nitrogen or preserved in RNAlater tissue buffer or 95% ethanol. Genomic DNA was extracted using a guanidine thiocyanate extraction protocol. We also extracted DNA from species of *Bradytriton, Dendrotriton, Nototriton, Nyctanolis,* and *Oedipina* as outgroups. Voucher information for samples used in phylogenetic analyses is given in Table S1. We sequenced fragments of two mitochondrial genes: the large subunit ribosomal RNA gene (16S) and cytochrome b (cytb).

We also sequenced fragments of four nuclear genes: brain-derived neurotrophic factor (BDNF), proopiomelanocortin (POMC), recombination-activating gene 1 (RAG1), and solute carrier family 8 member 3 (SLC8A3). Primer combinations, PCR conditions, and alignment lengths are given in Table S2. PCR products were cleaned using 2 µL of 1:5 diluted ExoSAP-IT (USB Corporation, Cleveland, OH), cycle sequenced, purified using Sephadex and run on an ABI-3730 capillary sequencer (Applied Biosystems, Foster City, CA). Sequences were edited using Geneious v5.6.5 (Drummond *et al.*, 2010); GenBank accession numbers are given in Table S3.

PHYLOGENETIC ANALYSIS

We aligned sequences for each gene using MUSCLE v3.8.3 (Edgar, 2004) and trimmed alignments to the point where a majority of individuals had sequence data. We estimated gametic phase for nuclear loci computationally using PHASE 2.1 (Stephens, Smith & Donnelly, 2001) and tested for recombination using the DSS test in TOPALi v2.5 (Milne *et al.*, 2009). No intralocus recombination was detected for any locus. We estimated genetic distance between haplotypes using the General Time Reversible (GTR) model (Tavaré, 1986) in the program PAUP* (Swofford, 2003).

We divided all protein-coding genes into data blocks by codon position and used PartitionFinder v1.0.1 (Lanfear *et al*., 2012) to test different partition schemes and select substitution models for each partition. We ran PartitionFinder separately for the mitochondrial and nuclear genes because of ploidy differences, using the greedy algorithm and the Bayesian Information Criterion (BIC) to choose between partitioning schemes. For the mtDNA, the following partitioning scheme and substitution models were selected: 16S + cytb codon position 1 – GTR+G; cytb position 2 – HKY+I; cytb position 3 – GTR+G. For nuclear data, the partitioning scheme and models were: BDNF codon position 1 + RAG1 position 2 + SLC8A3 position 2 – F81+G; BDNF position 2 + POMC position 3 + SLC8A3 position 3 – K80+G; BDNF position 3 + POMC positions 1 and 2 + RAG1 position 1 + SLC8A3 position 1 – HKY+G; RAG1 position 3 – K80+G. These partitioning schemes and substitution models were used for all subsequent analyses.

We estimated a mitochondrial gene tree using both maximum likelihood (ML) and Bayesian inference (BI). ML analysis was done using RAxML v7.2 (Stamatakis, 2006) run on the CIPRES portal (Miller, Pfeiffer & Schwartz, 2010), with a separate GTR+G model for each partition (RAxML does not include less complex models) and 1000 bootstrap replicates. Bayesian phylogenetic inference was done using MrBayes 3.2 (Ronquist *et al*., 2012), run for 2×10^7 generations, sampled every 1000 generations, with the first 5000 samples discarded as burn-in. We also estimated a phylogeny using a concatenated matrix of the mtDNA and nuclear genotype data using these two programs with the same MCMC run parameters as for the mtDNA analysis, as well as from a matrix of the concatenated nuclear data only. We estimated haplotype networks for nuclear loci using TCS v. 1.2 (Clement, Posada & Crandall, 2000), with a probability threshold of 0.90.

We used *BEAST v1.7.4 (Heled & Drummond, 2010) to estimate a species tree with nuclear loci only; analyses with mtDNA and nuclear loci failed to converge, perhaps because of differences between the topology of the mtDNA gene tree and concatenated phylogeny (see Results). *BEAST coestimates gene and species trees under a multispecies coalescent model, and requires *a priori* assignment of individuals to species. Based on similarity in mtDNA sequence and external morphology, several individuals from the Sierra de Xucaneb, Alta Verapaz that could not be reliably classified to named species were included as a separate species, and a single individual of uncertain species identification (from Bethel, Alta Verapaz; Fig. 1) was included as its own species to allow subsequent analyses of the distinctiveness of these taxa with coalescent species delimitation methods. Among-branch rate variation was modelled using a relaxed lognormal clock

for each partition, and we used a Yule tree prior for the species tree. We ran two separate analyses of 2×10^8 generations each, sampled every 10 000 generations, and the first 5000 samples were discarded as burn-in; the two runs were combined using LogCombiner (Drummond & Rambaut, 2007) to estimate a consensus tree. We assessed convergence by examining the posterior probability trace in Tracer v1.5, and checked that all effective sample size values for parameters were > 200.

SPECIES DELIMITATION

Although all described species of *Cryptotriton* are distinguishable based on external morphology, and many have osteological differences, these differences are often small and difficult to distinguish without statistical analysis. This has made species delimitation a particular challenge for the group; in other genera of small-bodied tropical salamanders, molecular data have proven key to first identifying lineages that serve as the units for subsequent morphological comparison (Hanken, 1983; Darda, 1994). In cases where differences in external morphology and osteology between lineages identified using molecular data are small, and levels of genetic divergence between lineages are near the level expected seen between different species in the same group, coalescent species delimitation methods (Yang & Rannala, 2010) provide an additional tool that can be used for taxonomy.

We used the program BPP 2.2 (Rannala & Yang, 2013) to test the hypothesis that one or both of the groups of populations from Alta Verapaz (from the Sierra de Xucaneb and Bethel) represent distinct, undescribed species. BPP uses a reversible jump Markov Chain Monte Carlo (rjMCMC) algorithm to move between states where sister species are combined into a single species, or a single species is split into two sister species. This algorithm requires a guide tree, and the choice of guide tree can have a major impact on results because it controls which combinations of species can be merged into a single species at any point in the analysis. We used the species tree estimated from *BEAST analysis of nuclear loci, which placed both of these taxa in a group with *Cryptotriton veraepacis*, with the single individual from Bethel, Alta Verapaz as the sister taxon to *C. veraepacis*. This individual from Bethel is more similar in ventral coloration to the other, more eastern Alta Verapaz populations than it is to *C. veraepacis* (see Results), so we also used an alternative guide tree matching the *BEAST topology except with the two lineages from Alta Verapaz as sister taxa. For each tree, we used species delimitation algorithm 1 (Yang & Rannala, 2010) to test three combinations of prior distributions. Both population size (θ) and root divergence time (τ_0) are modelled using a gamma distribution, $G(\alpha, \beta)$, with

the α and β parameters set by the user. Following Leaché & Fujita, (2010), we tested parameter combinations representing: deep divergence time and large ancestral population size ($\theta \sim G(1, 10)$; $\tau_0 \sim G(1, 10)$), shallow divergence time and small ancestral population size ($\theta \sim G(2, 2000)$; $\tau_0 \sim G(2, 2000)$), and shallow divergence time with large ancestral population size ($\theta \sim G(2, 2000)$; $\tau_0 \sim G(1, 10)$). Each analysis was run for 500 000 generations, sampled every five generations, with the first 50 000 generations discarded as burn-in. All analyses used a starting tree with all taxa merged into a single species. Each set of prior combinations, loci (all vs. nuclear only), and guide tree was run with either a species model prior of uniform labelled histories or with a user-defined set of prior probabilities on splits. In the latter case, we set the prior probability of all splits except those between *C. veraepacis*, the eastern Alta Verapaz populations, and the Bethel population, as well as the split between *C. nasalis* and *C. necopinus*, to 1.0, with the prior probability of these remaining splits set to 0.5. This approach was used to account for the fact that named species of *Cryptotriton* are clearly distinct species based on both morphological and phylogenetic grounds; we tested *C. nasalis* and *C. necopinus* because *C. necopinus* is known only from a single specimen and is somewhat morphologically similar to *C. nasalis*. The analyses with user-defined prior probabilities of splits used a starting tree with *C. nasalis* and *C. necopinus* merged into one species, and *C. veraepacis* and all populations from Alta Verapaz merged into a single species.

BIOGEOGRAPHIC ANALYSES

We used the program LAGRANGE 2.0 (Ree & Smith, 2008a) to estimate the pattern of range evolution and ancestral distribution of *Cryptotriton*. LAGRANGE implements a Dispersal-Extinction-Cladogenesis (DEC) model in a ML framework, in which taxa are distributed in discrete areas. Along branches, a species can either disperse to a new area, go extinct in an area it inhabits, or experience a cladogenesis event. In the DEC model, when cladogenesis occurs, one daughter species inherits a single area from the range of the parental species, and the other daughter species inherits either the remainder or entirety of the parental species' range (Ree *et al*., 2005; Ree & Smith, 2008b). We divided the study region into three areas: (1) the highlands of the Maya block, from the Sierra de Santa Cruz and Sierra de Xucaneb, Guatemala northwest into Chiapas, (2) the Motagua fault zone and Guatemalan Volcanic Cordillera, between the Chortís and Maya highlands, and (3) the Chortís highlands, extending from the Motagua fault east (Fig. 1) (Marshall, 2007). The Motagua fault zone includes the Sierra de las Minas, Sierra de Chuacús, and other highland areas at the intersection of the Chortís and Maya blocks, north of the Motagua Valley and south of the Polochíc Valley. We modelled range evolution on the *BEAST species tree and allowed a maximum range size of two areas. One of our outgroup taxa (*Nyctanolis pernix*) is found in both the Maya highlands and the Motagua fault zone, while none of the other species in our study is found in more than one of these areas. We allowed species to have only contiguous ranges, excluding a range composed of the Chortís and Maya highlands; no species of salamander is found in these two areas and not in the intervening Motagua fault zone.

MORPHOLOGICAL ANALYSES

We took the following 13 measurements from preserved museum specimens of *Cryptotriton* (Appendix) using either Vernier calipers or an ocular micrometer: distance from tip of snout to posterior angle of vent (SVL), tail length (TL), axilla-groin distance (AX), distance from tip of snout to gular fold (head length, SG), head width at widest point (HW), forelimb length (FLL), hind limb length (HLL), right foot width (RFW), length of longest (third) toe (T3), length of fifth toe (T5), distance between external nares (IN), external nostril length along major axis (NL), and external nostril width along minor axis (NW). We counted ankylosed maxillary and premaxillary teeth (PMT) and vomerine teeth (VT), with counts summed for the right and left sides. We summed counts of maxillary and premaxillary teeth and compared the total number of teeth on the upper jaw (MT). We calculated the ratio of nostril width to nostril length (ratio of nostril dimensions, ND) as an index of nostril shape. We used the colour nomenclature and numbers of Köhler (2012) to describe the colour of specimens of *Cryptotriton*.

We had relatively few specimens of several species of *Cryptotriton*, due to the difficulty of finding these secretive organisms in the wild. We used a *t*-test with the two species for which we had large relatively series of both males and females, *C. sierraminensis* and *C. veraepacis*, to determine whether sexual dimorphism exists within species for the morphological characters we measured. The sex of each specimen was determined by examination of cloacal morphology. Only the number of premaxillary teeth differed significantly between sexes for both species after applying a Bonferroni correction for multiple comparisons (per comparison $\alpha = 0.0014$ for an overall α of 0.05). Due to the lack of significant sexual dimorphism in the measured characters for these two species, we combined data for males and females for all subsequent morphological comparisons.

RESULTS

The mitochondrial gene tree estimated using both ML and Bayesian inference shows almost no support for relationships between species of *Cryptotriton*. The monophyly of *Cryptotriton* is strongly supported (Fig. 2), and *Cryptotriton alvarezdeltoroi* is estimated to be the sister taxon of a clade containing all other species of *Cryptotriton*, but with low support (bootstrap support [BS] = 28, Posterior Probability [PP] = 0.86). The single sample from Bethel is strongly supported as the sister taxon of *C. veraepacis*, and the three other samples from the Sierra de Xucaneb, Alta Verapaz are strongly supported as a clade. The average pairwise GTR distance between sequences from the two sites in the Sierra de Xucaneb is moderate (16S: 0.018, cytb: 0.033), while the average pairwise GTR distance between the Sierra de Xucaneb samples and *C. veraepacis* is larger (16S: 0.053, cytb: 0.14). All other relationships are either unresolved or poorly supported. The sister taxon of *Cryptotriton* is not well supported in either tree. Analysis of all loci concatenated into a single data matrix also resolved *C. monzoni* as the sister taxon of a clade containing all remaining species of *Cryptotriton* (Fig. S1). Within this clade, *C. nasalis* and *C. necopinus* were strongly supported as sister taxa, and *C. sierraminensis* was estimated to be the sister taxon of these two species. All other interspecific relationships were unresolved. The three samples from the Sierra de Xucaneb, Alta Verapaz formed a clade, as did *C. veraepacis* and the sample from Bethel. *Cryptotriton* was estimated to be the sister taxon of a clade containing *Bradytriton, Nototriton, Nyctanolis*, and *Oedipina*, but with weak support (BS = 23, PP = 0.91). In the concatenated nuclear results (Fig. S2), *C. monzoni* was again the sister species of a clade containing all other *Cryptotriton*. Relationships between *C. nasalis*, *C. necopinus*, and *C. sierraminensis* matched those in the tree from all loci concatenated, and *C. alvarezdeltoroi* received some support as the sister taxon of this clade (BS = 71, PP = 0.90). Samples from Alta Verapaz and *C. veraepacis* formed a clade, with relationships within this clade unresolved. *Cryptotriton* was again estimated to be the sister taxon of the clade containing all Central American endemic genera except *Dendrotriton*, with higher support than in analysis of all loci (BS = 0.58, PP = 0.91).

The *BEAST results from the nuclear loci provide little additional support for relationships between species compared to the mtDNA gene tree. *Cryptotriton monzoni* is estimated to be the sister taxon of a clade containing all remaining species of *Cryptotriton*, and *C. nasalis* and *C. necopinus* are strongly supported as sister species (Fig. 3). There is a strongly supported clade containing *C. veraepacis*, the populations from the Sierra de Xucaneb, Alta Verapaz, and the Bethel, Alta Verapaz population; within this clade, *C. veraepacis* and the

Bethel population are weekly supported as sister taxa. Nuclear haplotype networks show a fairly high degree of divergence between species (Fig. 4). Different species share haplotypes for only one locus, POMC; a single haplotype is shared between *C. veraepacis* and the species from Finca Volcán (green and cyan, respectively, in Fig. 4), and the latter shares one haplotype with the species from Bethel (cyan and blue, respectively, in Fig. 4). In all networks, *C. monzoni* is widely separated from haplotypes of all other species (by 6–16 mutational steps). Haplotypes from the Bethel individual are either most closely connected to haplotypes from the Sierra de Xucaneb, Alta Verapaz (BDNF, POMC, RAG1) or *Cryptotriton veraepacis* (SLC8A3).

Results of species delimitation using BPP with equal prior probability for labelled histories supported the most partitioned species tree in all cases, regardless of combinations of prior values or the guide tree used in the analysis. Using the *BEAST guide tree, *Cryptotriton* from the Sierra de Xucaneb, Alta Verapaz and Bethel were both supported as distinct species with PP > 0.99. Using the alternate guide tree in which these two populations as sister taxa, they were both supported as distinct species in all cases with PP > 0.97. When the user-defined prior probabilities of all splits were used, the results still strongly supported the most split species tree possible with PP > 0.97, regardless of the guide tree, prior combinations, or dataset used.

The LAGRANGE results (Fig. 5) estimated the ancestor of all extant species of *Cryptotriton* to have most likely occurred in the Chortís highlands and Motagua fault zone (relative probability = 0.73), or less probably in only the Chortís highlands (prob. = 0.24). The initial divergence event within the genus was estimated to have most likely occurred between the Chortís highlands and the Motagua fault zone plus Chortís highlands (relative probability = 0.57) or within the Chortís highlands (prob. = 0.24), with three scenarios involving both the Chortís highlands and Motagua fault zone being less probable. The ancestor of the remaining species of *Cryptotriton* excluding *C. monzoni* was estimated to have occurred in both the Chortís highlands and Motagua fault zone. The divergence between daughter lineages from this node was between the Chortís highlands and either the Motagua fault zone (prob. = 0.89) or the Chortís highlands and Motagua fault zone (prob. = 0.06), with the ancestor of *C. nasalis* and *C. necopinus* inheriting the Chortis highlands portion of the range (or, with low probability, the Chortís highlands and Motagua fault zone), and the remaining Guatemalan/Mexican species inheriting a range consisting of the Motagua fault zone. After the divergence between *C. sierraminensis* and the Alta/Baja Verapaz species plus *C. alvarezdeltoroi*, *C. sierraminensis* inherited a range of only the Motagua fault zone with the remaining species inheriting either a range of only
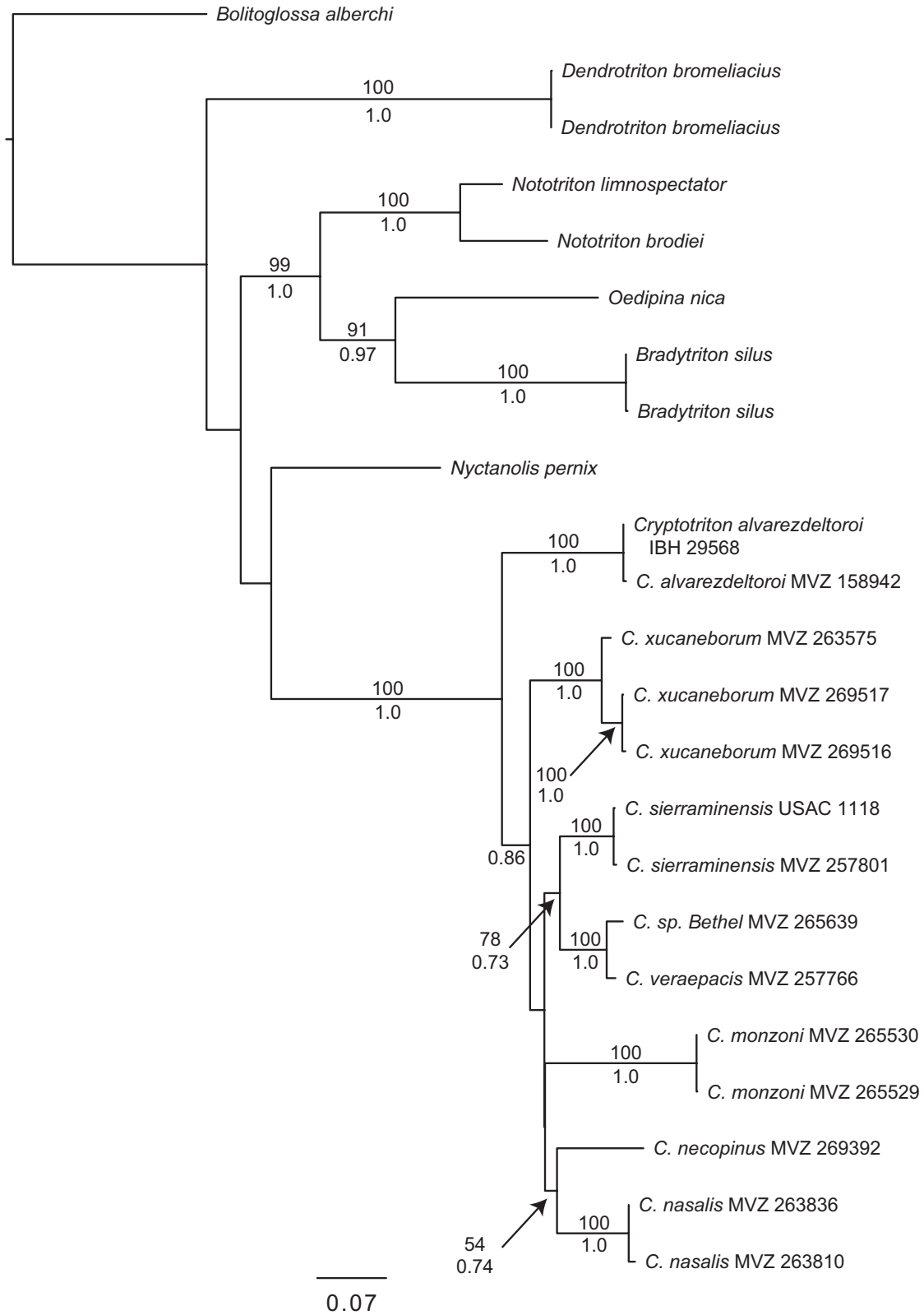
Figure 2. Mitochondrial gene tree from maximum likelihood (ML) analysis of 16S and cytb data. Numbers above branches are bootstrap support values from ML analysis, and numbers below branches are posterior probabilities from Bayesian analysis. Bootstraps below 50 and posterior probabilities below 0.5 are not shown.
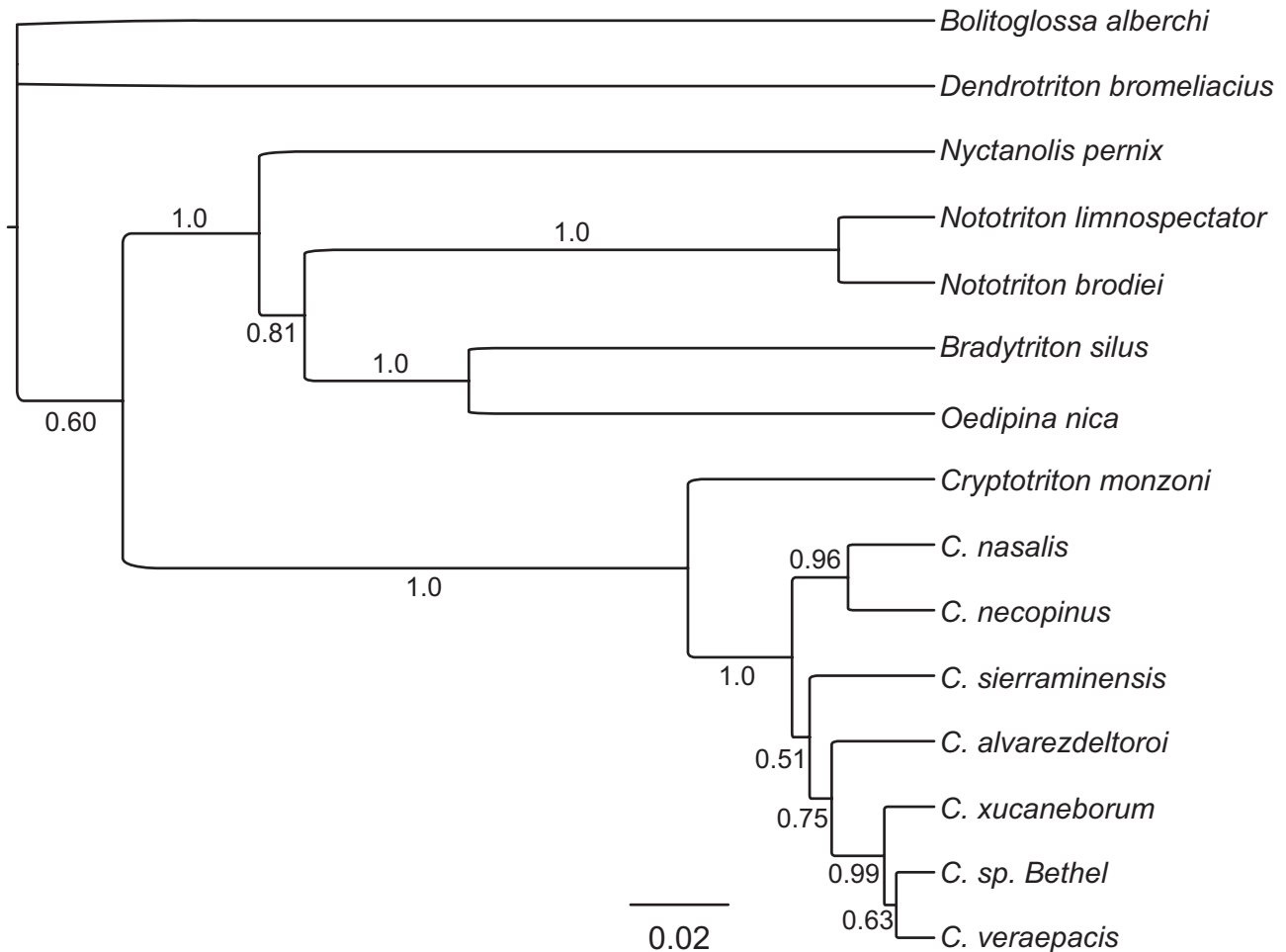
Figure 3. Species tree estimate from *BEAST analysis of nuclear loci. Numbers indicate posterior probability of clades.

the Motagua fault zone (prob = 0.74), Maya highlands (prob. = 0.13) or the both of these areas (prob. = 0.10). The divergence between *C. alvarezdeltoroi* and the three taxa from Alta and Baja Verapaz, Guatemala occurred either between the Maya highlands and the Maya highlands plus Motagua fault zone (prob. = 0.71), within the Maya highlands (prob. = 0.15), or less probably between these two areas or within the Motagua fault zone. Finally, the divergence between *C. veraepacis* and the Bethel population most likely occurred between the Maya highlands and the Maya highlands plus Motagua fault zone (prob. = 0.87), or within the Maya highlands (prob. = 0.10).

All species of *Cryptotriton* resemble each other closely in external morphology, but we found some differences between the populations from the Sierra de Xucaneb, Alta Verapaz and described species in characters including tail length, foot width, and nostril size (Table 1). Based on differences in external morphology, osteology, and mtDNA sequence, as well as on the results of the coalescent species delimitation, we find

that the populations from eastern Alta Verapaz formerly referred to *Cryptotriton veraepacis* represent a distinct species of *Cryptotriton*.

CRYPTOTRITON XUCANEBORUM, NEW SPECIES

Sierra de Xucaneb Hidden Salamander
   Salamandra Escondida de la Sierra de Xucaneb
   Figures 6A, 6C
   Cryptotriton veraepacis McCranie and Rovito, 2014 (part)
   Cryptotriton veraepacis Vásquez-Almazán *et al*. 2009 (part)
   Cryptotriton veraepacis Lynch and Wake, 1978 (part)
   Holotype. – MVZ 263575, male, Guatemala, Departamento Alta Verapaz, Municipio Senahú, 3.8 km S (by road) Finca El Volcán, 15.46102 °N 89.87055 °W (WGS84 datum), 1370 m, 19 August 2007, S. M. Rovito, C. R. Vásquez-Almazán, E. G. Ruano-Fajardo, and T. J. Papenfuss.
   Paratypes. – (*n* = 4). Three females, MVZ 269516–269517, USAC 3496, one male, USAC 3497,
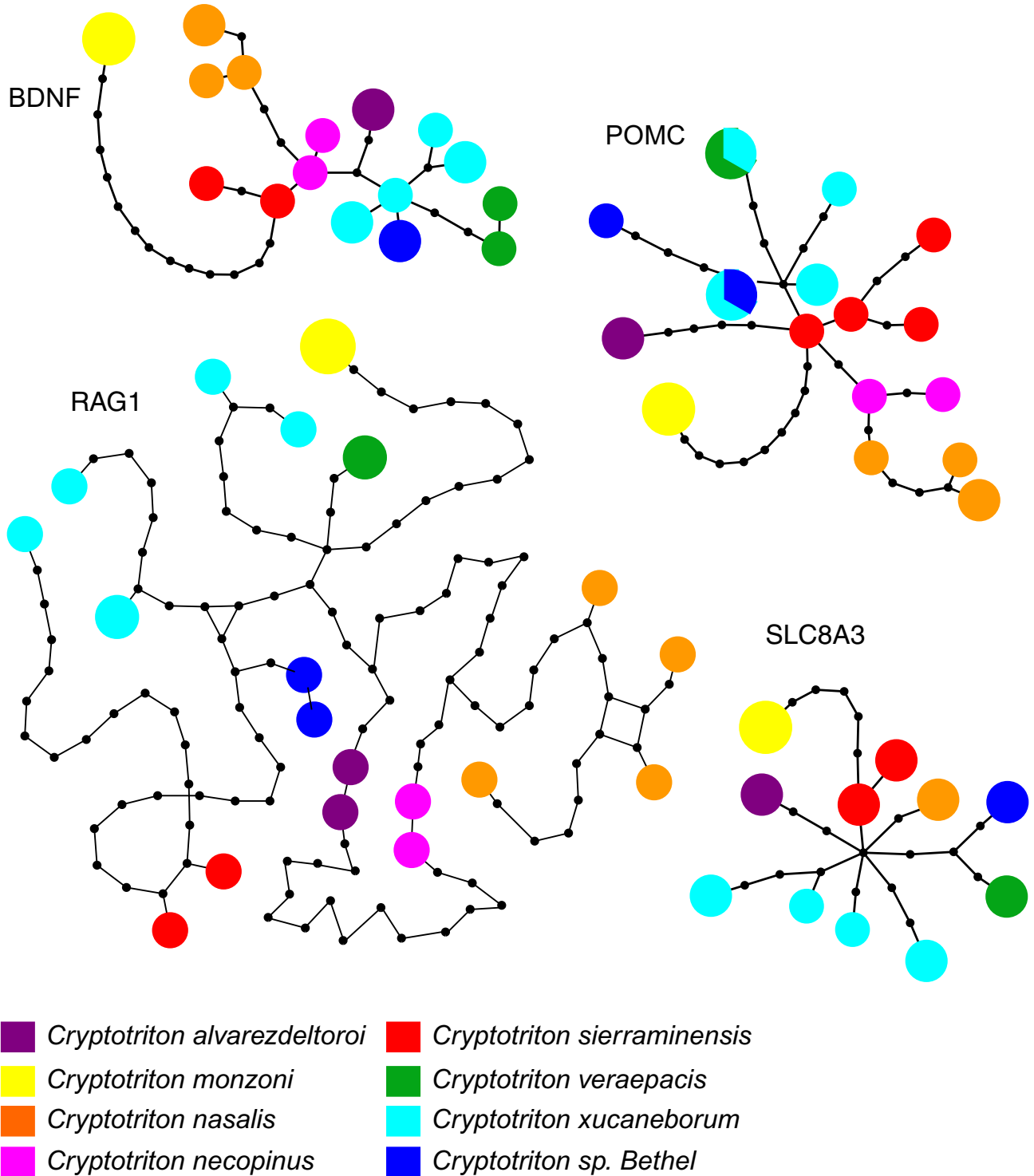
Figure 4. Haplotype networks from TCS analysis of nuclear loci. Size of circle is proportionate to the frequency of each haplotype. Black dots represent inferred haplotypes not observed in sequence data, and lines connect haplotypes separated by a single mutational step.
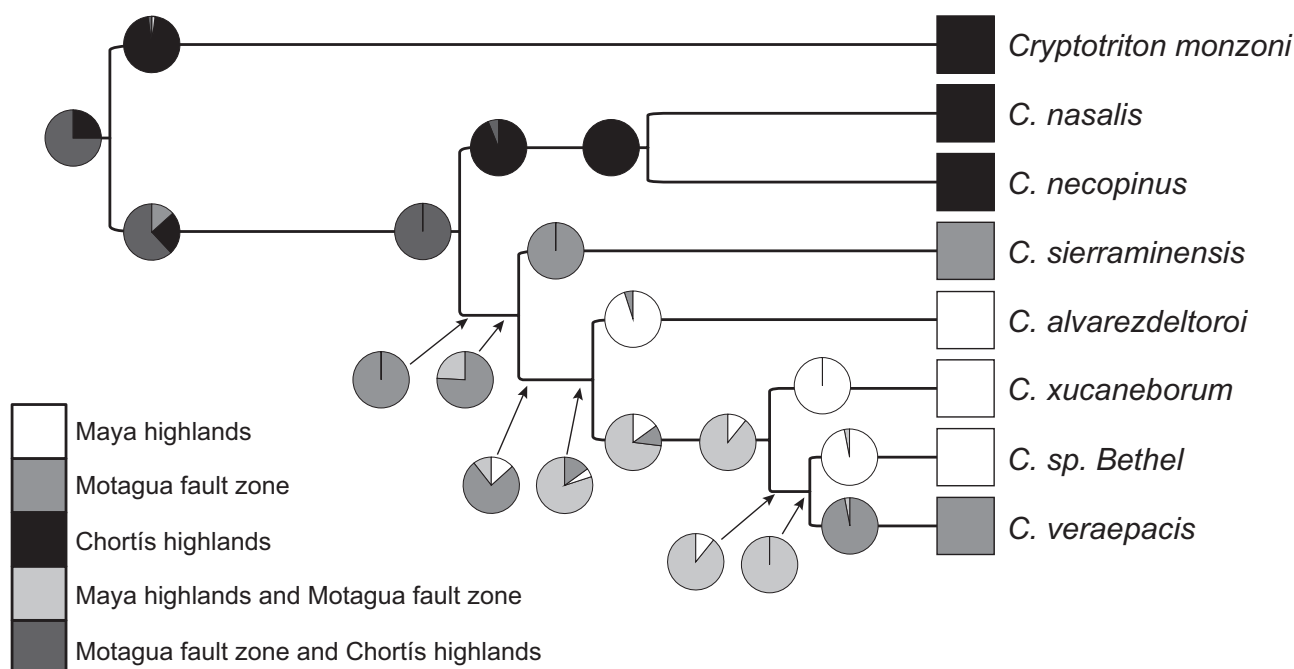
Figure 5. Results of LAGRANGE analysis of geographic range evolution of *Cryptotriton*. Results for other genera are not shown. Pies at nodes are colored by the relative probability of each geographic range combination, and squares at tips show the areas currently occupied by each species. Each node has a pie representing the range of the ancestor prior to the speciation event and two pies representing the range of each daughter species immediately after the speciation event.

Guatemala, Alta Verapaz, Municipio Tucurú, Chelemhá Reserve, 15.3558 °N, 90.0775°W (WGS84 datum), 2045 m.

Referred specimens. – ANSP 28198, ANSP 28199.

Diagnosis. – Distinguished by its very dark grey ventral coloration from *Cryptotriton sierraminensis* (yellow) and *C. veraepacis* (lighter grey); gular coloration darker than in *C. veraepacis*, with no yellow (some yellow in *C. sierraminensis*) (Vásquez-Almazán *et al.*, 2009). Distinguished from *C. veraepacis* and *C. sierraminensis* by lack of a tibial spur, and from *C. sierraminensis* by having prefrontal pierced by nasolacrimal duct, rather than evacuated along anterior margin and by the lack of a postorbital vomerine process (Vásquez-Almazán *et al.*, 2009). Distinguished from *C. necopinus* by having prefrontal processes of the premaxillary that arise fused and separate distally, rather than arising separately (McCranie & Rovito, 2014), and by having a longer tail, more rounded nostrils, a wider foot, and fewer maxillary and vomerine teeth (Table 1). Distinguished from *C. nasalis* by having a prefrontal bone pierced by the nasolacrimal duct, rather than evacuated along the anterior margin (Lynch & Wake, 1978) and smaller nostrils (Table 1). Distinguished from *C. alvarezdeltoroi* by its larger size and smaller nostrils (Table 1).

Description of holotype. – A relatively small adult male (SVL = 25.7 mm). Head moderately sized, ap-proximately same width as body, snout truncate. Eyes extend slightly beyond margin of jaw. Paratoid glands large, relatively well defined. Nostrils large (maximum nostril diameter = 0.6 mm). Well developed hands and feet with little webbing between digits; tips of digits rounded. Limbs relatively long; adpressed limbs separated by approximately two costal folds. Tail longer than body (37.4 mm), approximately rounded in cross-section, constricted at base, gradually tapering to a point. Nasolabial protuberances well developed and wide but not long, extend slightly beyond margin of lip. Large, elliptical mental hedonic gland present. Maxillary teeth (38) small and relatively numerous; premaxillary teeth (3) large, pierce upper lip. Relatively few vomerine teeth (8), arranged in line extending to internal margin of choanae.

Measurements of the holotype (in mm) and tooth counts. – Head width 3.6; snout to gular fold (head length) 5.0; head depth at posterior angle of jaw 2.2; eyelid length 1.8; eyelid width 0.7; anterior rim of orbit to snout 0.9; horizontal orbit diameter 2.2; interorbital distance 1.3; snout to forelimb 7.7; distance separating external nares 0.8; snout projection beyond mandible 0.7; snout to posterior angle of vent (SVL) 25.7; snout to anterior angle of vent 33.7; axilla to groin 13.0; tail length 37.4; tail width at base 1.8; tail depth at base 2.3; forelimb length 5.4; hind limb length 6.5; width of right manus 1.4; width of right pes 2.3; length of

Table 1. Means, standard deviations, and ranges for specimens measured for morphological comparisons. Total number of specimens examined is given with species name; number noted for each measurement when different from total

|	*C. alvarezdeltoroi* N = 3	*C. monzoni* N = 3	*C. nasalis* N = 5	*C. necopinus* N = 1	*C. sierraminensis* N = 45	*C. veraepacis* N = 18	*C. xucaneborum* N = 5
SVL	24.4 ± 3.81 (20.0–26.6)	22.6 ± 0.52 (22.3–23.2)	27.8 ± 1.58 (25.6–29.5)	26.4	27.8 ± 3.15 (22.2–35.4)	28.1 ± 2.19 (25.2–32.2)	27.8 ± 2.83 (24.9–32.0)
TL	28.2 ± 3.57 (25.1–32.1)	24.8 ± 1.89 (23.1–26.7)	31.9 ± 1.26 (30.6–34.0)	26	30.0 ± 7.04 (14.9–43.7) N = 39	37.9 ± 3.94 (33.4–44.9)	33.7 ± 3.38 (28.8–37.4)
AG	13.4 ± 2.51 (10.5–15.2)	12.3 ± 0.71 (11.8–12.8) N = 2	14.7 ± 1.14 (12.8–15.7)	13.7	14.6 ± 1.62 (11.0–19.4)	14.6 ± 1.18 (13.0–16.8)	15.1 ± 2.33 (13.0–18.7)
SG	4.7 ± 0.79 (3.8–5.3)	4.3 ± 0.40 (4.1–4.8)	5.6 ± 0.2 (5.4–5.8)	5.3	5.6 ± 0.56 (4.2–6.7)	5.8 ± 0.49 (4.8–6.5)	5.5 ± 0.57 (5.0–6.4)
HW	3.7 ± 0.44 (3.2–4.0)	3.3 ± 0.06 (3.2–3.3)	4.2 ± 0.24 (3.9–4.5)	3.4	3.9 ± 0.37 (3.2–4.8)	4.1 ± 0.4 (3.4–4.7)	3.8 ± 0.39 (3.5–4.4)
FLL	4.8 ± 1.17 (3.5–5.8)	4.6 ± 0.35 (4.2–4.9)	5.9 ± 0.53 (5.4–6.8)	5.3	5.4 ± 0.65 (3.9–6.9)	5.6 ± 0.69 (3.7–6.7)	5.7 ± 0.74 (5.1–7.0)
HLL	5.5 ± 1.08 (4.3–6.3)	5.1 ± 0.31 (4.8–5.4)	6.8 ± 0.69 (5.9–7.5)	6.8	6.0 ± 0.91 (4.2–8.8)	6.6 ± 0.81 (4.9–8.3)	6.8 ± 0.7 (6.0–7.9)
RFW	1.9 ± 0.33 (1.5–2.1)	1.5 ± 0.1 (1.4–1.6)	2.4 ± 0.11 (2.3–2.6)	1.3	2.4 ± 0.46 (1.5–3.6) N = 44	2.8 ± 0.45 (2.0–3.4)	2.2 ± 0.56 (1.7–3.1)
IN	0.91 ± 0.03 (0.88–0.96)	0.94 ± 0.03 (0.92–0.96) N = 2	0.95 ± 0.12 (0.85–1.14)	0.3	0.79 ± 0.10 (0.60–1.0)	0.82 ± 0.10 (0.60–1.0)	0.69 ± 0.19 (0.40–0.89)
T3	0.66 ± 0.04 (0.62–0.70) N = 2	0.59 ± 0.07 (0.54–0.64) N = 2	1.04 ± 0.15 (0.94–1.3)	1.9	0.90 ± 0.12 (0.60–1.1) N = 38	0.89 ± 0.11 (0.8–1.2)	1.01 ± 0.37 (0.6–1.5)
T5	0.32 ± 0.02 (0.30–0.34) N = 2	0.17 ± 0.04 (0.14–0.20) N = 2	0.60 ± 0.08 (0.48–0.68)	1.6	0.46 ± 0.05 (0.34–0.60) N = 34	0.44 ± 0.10 (0.3–0.6)	0.54 ± 0.25 (0.2–0.9)
NL	0.60 ± 0.07 (0.50–0.66)	0.53 ± 0.04 (0.50–0.56) N = 2	0.66 ± 0.01 (0.64–0.67)	0.8	0.62 ± 0.05 (0.52–0.80)	0.62 ± 0.05 (0.58–0.76)	0.50 ± 0.03 (0.48–0.54) N = 3
NW	0.51 ± 0.01 (0.50–0.52)	0.45 ± 0.04 (0.42–0.48) N = 2	0.54 ± 0.05 (0.48–0.60)	0.5	0.47 ± 0.04 (0.40–0.6)	0.50 ± 0.04 (0.44–0.56)	0.41 ± 0.06 (0.34–0.46) N = 3
ND	1.18 ± 0.16 (1.00–1.28)	1.18 ± 0.02 (1.17–1.19) N = 2	1.22 ± 0.12 (1.10–1.40)	1.60	1.33 ± 0.11 (1.08–1.60)	1.26 ± 0.11 (1.11–1.50)	1.24 ± 0.15 (1.14–1.41) N = 3
PMT+MT	44.0 ± 15.62 (26–54)	32.7 ± 15.04 (23–50)	53.0 ± 2.92 (49–56)	59	50.8 ± 6.37 (37–61) N = 43	48.9 ± 6.61 (35–59)	45.8 ± 7.56 (37–57)
VT	9.0 ± 1.00 (8–10)	8.3 ± 0.58 (8–9)	11.2 ± 1.79 (9–14)	23	10.2 ± 1.98 (4–15) N = 44	9.1 ± 1.32 (8–12)	9.0 ± 2.65 (6–13)
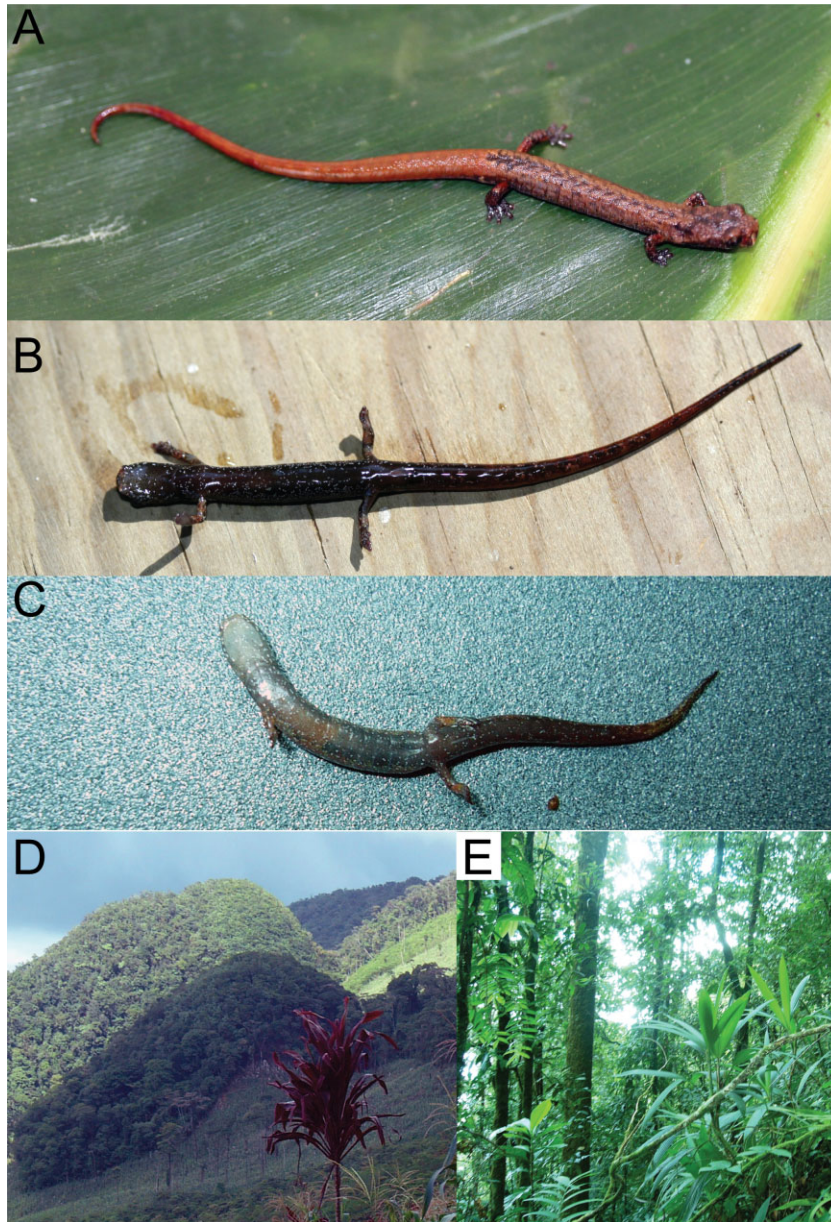
Figure 6. (A) Holotype of *Cryptotriton xucaneborum* in life. (B) Ventral view of holotype showing dark grey ventral coloration. (C) Ventral view of an individual of *C. veraepacis* (USAC 1920) showing lighter grey ventral coloration. (D) View of type locality of *C. xucaneborum*, showing small forest fragment surrounded by agricultural land. (E) Habitat where holotype of *C. xucaneborum* was collected.

longest toe 1.2; length of shortest toe 0.1; maximum nostril diameter 0.6; shoulder width 2.5. Maxillary teeth 38, premaxillary teeth 3, vomerine teeth 8.

Coloration of the holotype in life (based on photos). – Numbers in parentheses refer to colours from Köhler (2012). Dorsal surface of head Flesh Ocher (57) with Burnt Umber (48) in the centre of head from intercanthal region to just anterior to insertion of forelimbs. Dorsal surface of body Salmon Colour (58) with a suggestion of Dark Yellow Buff (54). Chevrons of Burnt Umber (48) along dorsal midline from insertion of forelimbs to base of tail. Dorsal surface of tail uniform Dark Salmon Colour (58), becoming more reddish along final third of tail. Dorsal surface of limbs Light Pratt's Rufous (71) and Salmon Colour (58) with Dark Drab (45) speckles and white flecks. Dorsal surface of feet Light Neutral Grey (297) with white flecks; toe tips pinkish. Lateral surface of head and body with same background colours as above, blending ventrally into Dark Greyish Brown (284) with numerous white flecks. Gular region mottled

Light Neutral Grey (297) and Sepia (286), becoming nearly uniform Sepia just anterior to gular fold. Ventral surface of body and anterior third of tail Sepia. White flecks on gular region and ventral surface of body and tail, becoming less numerous toward ventral midline. Posterior two-thirds of tail Vinaceous (247), with some Sepia; white flecks throughout tail. Ventral surfaces of limbs Pale Neutral Grey (296) with Tawny Olive (17), small white flecks. Underside of feet Pale Neutral Grey, toe tips pinkish.

Colour of the holotype in alcohol. – Dorsal surface of head Raw Umber (22), with Hair Brown (277) in the centre of head from intercanthal region to just anterior to insertion of forelimbs. Dorsal surface of body Raw Umber with Hair Brown chevrons along dorsal midline. Dorsal surface of tail Buff (5). Dorsal surface of limbs and feet mottled Buff and Raw Umber (23). Gular region mottled Drab-Grey (256) and Hair Brown, becoming nearly all brown towards gular fold. Ventral surface of body Hair Brown. Anterior third of tail Hair Brown, mottled with Buff towards tip. Underside of limbs Buff mottled with Hair Brown, underside of feet Smoke Grey (266). Pale flecks throughout ventral surface of head, body, and tail.

Variation – The male paratype is roughly the same size as the holotype (24.9 mm), while the three female paratypes are slightly larger, reaching a maximum of 32 mm. There is some variation in maxillary teeth in the type series, with the largest female having only 37 maxillary-premaxillary teeth, while another female has a total of 57 maxillary-premaxillary teeth. Similar variation is seen in the vomerine tooth counts; the largest female has only six vomerine teeth, while the smallest male has the most vomerine teeth (13). The female paratypes have nasolabial protuberances that are only very slightly developed and visible only as a slight swelling in the labial margin.

Osteology. – We examined X-rays of the holotype and a paratype (MVZ 269516). Prefrontal bones appear to be pierced by a nasolacrimal duct, as in *C. veraepacis* and the single known specimen of *C. necopinus* (Lynch & Wake, 1978; McCranie & Rovito, 2014). Frontal processes of premaxillary bone arise fused and separate distally. Vomer lacks a postorbital process. Tibial spur absent. As in other species of *Cryptotriton*, septomaxillary absent and mesopodials unmineralized. Phalangeal formula for manus is 1-2-3-2 and 1-2-3-3-2 for pes, identical to that of other species in the genus *Cryptotriton*.

Habitat and distribution. – Known only from two localities separated by 22 km in the Sierra de Xucaneb, Alta Verapaz, Guatemala. The species may occur at a few other points of relatively high elevation in the Sierra de Xucaneb, but extensive deforestation in most areas has eliminated what may have once been suitable habitat for the species. The holotype was found in an arboreal bromeliad, while the four paratypes from Chelemhá were found active at night on vegetation 1–2 m above the ground. The forest at Finca Volcán represents a transition from lower elevation forest to cloud forest, with relatively few bromeliads and other epiphyte growth, and is classified as subtropical rainforest (Holdridge, 1967), while habitat at Chelemhá is lower montane rain forest (Holdridge, 1967) with typical cloud forest vegetation and extensive epiphyte cover. The only syntopic species of salamander known to occur with *Cryptotriton xucaneborum* is *Bolitoglossa helmrichi*, which occurs at both known sites.

DISCUSSION

Our phylogenetic results, regardless of the method used, provide little support for the relationships between species of *Cryptotriton*. The mtDNA gene tree essentially shows a basal polytomy between all species. The *BEAST species tree is somewhat better supported, with *C. monzoni* clearly supported as the sister taxon to all other species in the genus. *Cryptotriton nasalis* and *C. necopinus* are also strongly supported as sister species and a clade of *C. veraepacis, C. xucaneborum*, and the Bethel population is well supported. Our results show that many of the internal branches within *Cryptotriton* are short, making the phylogeny of the group, and particularly the branching order towards the base of the *Cryptotriton* clade, difficult to estimate with confidence.

The placement of *C. monzoni* as the sister taxon of all remaining *Cryptotriton* in the *BEAST species tree (Fig. 3) and analyses of concatenated data (all loci or nuclear only; Figs S1–S2), along with the separation of *C. monzoni* from all other species in the nuclear haplotype networks for all loci (Fig. 4) is unexpected, as there appears to be no strong geographic barrier separating it from the other species distributed on the Chortís geological block (*C. nasalis* and *C. necopinus*). The ranges of *C. monzoni* and *C. nasalis* are both within the Sierra del Merendón, although the Sierra is composed of somewhat isolated mountain ranges separated by lower elevation areas. Of the species found near to or in sympatry with *C. nasalis*, only *Bolitoglossa diaphora* and *Oedipina tomasi* are not found near the type locality of *C. monzoni*. The other salamander species found in sympatry with *C. monzoni* (*B. conanti*, *B. dofleini, B. mexicana*, and *B. nympha*) are found in sympatry with or near localities of *C. nasalis*. Some of these species (*B. dofleini, B. mexicana, B. nympha*) are found at lower elevations and might be more able to disperse across low-elevation barriers between mountains, and *B. conanti* is larger than any *Cryptotriton*, suggesting greater capacity for dispersal. Still, the similarity in the salamander fauna of the sites where *C. monzoni* and *C. nasalis* are found indicates some

historical connectivity between the two sites, making the small ranges and isolation of *Cryptotriton* at each site the exception among salamanders in the area. *Cryptotriton* species appear to be more strictly limited to cloud forest than these *Bolitoglossa* species, and may be more susceptible to range fragmentation because of this habitat specificity.

The LAGRANGE results suggest that ancestor of all extant species of *Cryptotriton* occurred in the Chortís highlands, and most likely across the Motagua fault in Guatemala as well. The first two divergences in the phylogeny involve these two areas, showing their initial importance in the biogeographic history of the genus. The clade containing the non-Chortís highland species (*C. alvarezdeltoroi*, *C. sierraminensis*, *C. veraepacis, C. xucaneborum*, and the Bethel population) was estimated to have been distributed initially in the Motagua fault zone, with a dispersal even to the Maya block most likely occurring after the divergence of *C. sierraminensis* from the other species. The Maya highlands only become important in the biogeographic evolution of the group after the divergence of *C. sierraminensis*, and the Motagua fault zone was also estimated as part of the range of most nodes that included the Maya highlands in their estimated range. Taken together, these results show that the primary foci of divergence within this genus of salamanders were the Chortís highlands and Motagua fault zone, with a subsequent dispersal to the Maya highlands. While these biogeographic results depend on the underlying phylogeny used (in this case, the *BEAST species tree), the initial split within *Cryptotriton* between *C. monzoni* and the rest of the species in the genus is supported by multiple analyses. Given that initial split should have a strong impact on the biogeographic reconstruction of the origin of the genus (as one branch leads to a single species found only in one of the geographic areas used in the model), our inferences about the geographic origins of the genus should be robust to the choice of phylogenetic tree we used.

These biogeographic results stand in contrast to those from another arboreal salamander genus, *Dendrotriton*. The two genera are morphologically and ecologically similar, and were both contained within the same genus until *Dendrotriton* was recognized primarily based on differences in osteology (Wake & Elias, 1983). Both *Dendrotriton* and *Cryptotriton* primarily inhabit arboreal bromeliads in cloud forest habitat, and have the long tails and slender bodies typical of arboreal salamander species. *Dendrotriton* achieves highest species diversity in the Maya highlands, with only a single species found in the Guatemalan Volcanic Cordillera and another species found on the isolated Montaña de Santa Bárbara in the Chortís highlands. Biogeographic analyses with LAGRANGE indicated that *Dendrotriton* most likely arose in the Sierra Madre de Chiapas and/or the Sierra de los Cuchumatanes, both part of the Maya highlands, and subsequently dispersed to the Chortís highlands (Rovito *et al*., 2012). Even though three species of *Cryptotriton* are found in the Maya highlands, two of these are from Alta Verapaz and are very close to the Motagua fault zone; no *Cryptotriton* is known from the Sierra de los Cuchumatanes or the Sierra Madre de Chiapas. Only *C. alvarezdeltoroi* is found in the core of the Maya highlands. The contrasting biogeographic histories of these morphologically and ecologically similar genera, coupled with the fact that they are not known to occur in sympatry, suggests that they may have each diversified in a different portion of the highlands of Nuclear Central America, with subsequent diversification in the remaining highlands limited by the presence of the other genus.

The single specimen from Bethel, an isolated cloud forest patch north of San Pedro Carchá, Alta Verapaz, resembles both *Cryptotriton veraepacis* and *C. xucaneborum* in external morphology. It shares the darker ventral coloration with *C. xucaneborum*, yet differs from the few available specimens of that species by having more oblong nostrils (rather than nearly round), and in having a longer tail and shorter trunk relative to its body size. The Bethel specimen has a 16S sequence that is very similar to that of *C. veraepacis* (GTR distance = 0.008) and a cytb sequence that is also somewhat similar to that of *C. veraepacis* (GTR distance = 0.033), yet shares a haplotype with *C. xucaneborum* for POMC and has distinct haplotypes not shared with other species for the remaining three loci. The BPP analyses under all prior combinations and both guide trees suggest that it may warrant description as a distinct species. Alternatively, it may be assignable to either *C. veraepacis* or *C. xucaneborum*. If assignable to *C. veraepacis*, retention of ancestral polymorphism could be responsible for the sharing of nuclear haplotypes with *C. xucaneborum*. If the Bethel population is in fact assignable to *C. xucaneborum*, gene flow with *C. veraepacis* and mitochondrial capture could be responsible for the relatively small mtDNA distance between it and *C. veraepacis*. Additional species from Bethel will be necessary to examine morphological variation within this population and determine its taxonomic assignment.

The presence of another undescribed species of *Cryptotriton* in eastern Guatemala would not be surprising; all known species in the genus have small geographic ranges (Fig. 1). The complex topography of the region and the salamanders' reliance on cloud forest habitat may have caused multiple bouts of fragmentation or isolation in the past, promoting species divergence. Natural vicariance of montane forest habitat has driven divergence between populations and led to population structure within multiple species

(García-París *et al.*, 2000; Ruiz-Sanchez & Ornelas, 2014), and over longer timescales this could lead to species divergence. *Cryptotriton* and *Dendrotriton* are perhaps the most highly and obligatorily arboreal of all tropical salamander genera, with the exception of *D. cuchumatanus*, which occurs in high elevation oak forest with few or no bromeliads. All species of both genera are essentially microendemic, known from only a single site or several sites separated by only a few kilometres. The species with the largest range, *C. alvarezdeltoroi*, is known from few specimens and the single specimen that is somewhat distant from the type locality has not been examined genetically because of a lack of a tissue sample; thus, its taxonomic identification could be considered as tentative. This microendemism and rarity in collections can be a taxonomic hindrance, but also makes both of these genera excellent systems in which to study the impact of cloud forest distributional dynamics on diversification of animals. The discovery of additional populations of *Cryptotriton* in Nuclear Central America seems almost inevitable based on the rate of salamander species discovery in the region (Vásquez-Almazán *et al.*, 2009; Townsend *et al.*, 2010, 2011). Continued discovery and systematic studies of these cloud forest salamanders may help to resolve some parts of the phylogeny of *Cryptotriton*, and will improve our knowledge of how cloud forest distributions, geological events, and past climatic change have interacted to produce the high biodiversity and endemism observed in many Central American taxa.

ACKNOWLEDGEMENTS

REFERENCES

AmphibiaWeb. 2014. Information on Amphibian Biology and Conservation. Available at: http://www.AmphibiaWeb.org. Accessed 26 September 2014.

Bruijnzeel LA. 2001. Hydrology of tropical montane cloud forests: a reassessment. *Land Use and Water Resources Research* **1:** 1–18.

Campbell JA, Smith EN. 1998. New species of *Nototriton* (Caudata: Plethodontidae) from Eastern Guatemala. *Scientific Papers, Natural History Museum, University of Kansas* **6:** 1–8.

Clement M, Posada D, Crandall KA. 2000. TCS: a computer program to estimate gene genealogies. *Molecular Ecology* **9:** 1657–1659.

Darda DM. 1994. Allozyme variation and morphological evolution among Mexican salamanders of the genus *Chiropterotriton* (Caudata: Plethodontidae). *Herpetologica* **50:** 164–187.

Daza JM, Castoe TA, Parkinson CL. 2010. Using regional comparative phylogeographic data from snake lineages to infer historical processes in Middle America. *Ecography* **33:** 343–354.

Drummond AJ, Ashton B, Buxton S, Cheung M, Cooper A, Heled J, Kearse M, Moir R, Stones-Havas S, Sturrock S, Thierer T, Wilson A. 2010. Geneious 5.1. Available at: www.geneious.com.

Drummond AJ, Rambaut A. 2007. BEAST: Bayesian evolutionary analysis by sampling trees. *BMC Evolutionary Biology* **7:** 214.

Edgar RC. 2004. MUSCLE: a multiple sequence alignment method with reduced time and space complexity. *BMC Bioinformatics* **5:** 1–19.

Feder ME. 1982. Thermal ecology of neotropical lungless salamanders (Amphibia, Plethodontidae): environmental temperatures and behavioral responses. *Ecology* **63:** 1665–1674.

García-París M, Good DA, Parra-Olea G, Wake DB. 2000. Biodiversity of Costa Rican salamanders: implications of high levels of genetic differentiation and phylogeographic structure for species formation. *Proceedings of the National Academy of Sciences of the United States of America* **97:** 1640–1647.

García-París M, Wake DB. 2000. Molecular phylogenetic analysis of relationships of the tropical salamander genera *Oedipina* and *Nototriton*, with descriptions of a new genus and three new species. *Copeia* **2000:** 42–70.

Gentry AH. 1992. Tropical forest biodiversity: distributional patterns and their conservation significance. *Oikos* **63:** 19–28.

Good DA, Wake DB. 1993. Systematic studies of the Costa Rican moss salamanders, genus *Nototriton*, with descriptions of three new species. *Herpetological Monographs* **7:** 131–159.

Hamilton LS, Juvik JO, Scatena FN. 1995. *Tropical montane cloud forests*. New York, USA: Springer Verlag, 425.

Hanken J. 1983. Genetic variation in a dwarfed lineage, the Mexican salamander genus *Thorius* (Amphibia: Plethodontidae): taxonomic, ecologic and evolutionary implications. *Copeia* **1983:** 1051–1073.

Heled J, Drummond AJ. 2010. Bayesian inference of species trees from multilocus data. *Molecular Biology and Evolution* **27:** 570–580.

Holdridge LR. 1967. *Life zone ecology*. San Jose, Costa Rica: Tropical Science Center.

Jadin RC, Townsend JH, Castoe TA, Campbell JA. 2012. Cryptic diversity in disjunct populations of Middle American montane pitvipers: a systematic reassessment of *Cerrophidion godmani*. *Zoologica Scripta* **41:** 455–470.

Köhler G. 2012. *Color catalogue for field biologists*. Offenbach: Herpeton.

Lanfear R, Calcott B, Ho SY, Guindon S. 2012. PartitionFinder: combined selection of partitioning schemes and substitution models for phylogenetic analyses. *Molecular Biology and Evolution* **29:** 1695–1701.

Leaché AD, Fujita MK. 2010. Bayesian species delimitation in West African forest geckos (*Hemidactylus fasciatus*). *Proceedings: Biological Sciences* **277:** 3071–3077.

Luna-Vega I, Alcántara-Ayala O, Espinoza-Organista D, Morrone JJ. 1999. Historical relationships of the Mexican cloud forests: a preliminary vicariance model applying Parsimony Analysis of Endemicity to vascular plant taxa. *Journal of Biogeography* **26:** 1299–1305.

Lynch JF, Wake DB. 1978. A new species of *Chiropterotriton* (Amphibia: Caudata) from Baja Verapaz, Guatemala, with comments on relationships among Central American members of the genus. *Contributions in Science (Los Angeles)* **1978:** 1–22.

Marshall JS. 2007. The geomorphological and physiographic provinces of Central America. In: Bundschuh J, Alvarado GE, eds. *Central America: geology, resources and hazards*. Oxford: Taylor & Francis, 75–122.

McCranie JR, Rovito SM. 2014. New species of salamander (Caudata: Plethodontidae: *Cryptotriton*) from Quebrada Cataguana, Francisco Morazán, Honduras, with comments on the taxonomic status of *Cryptotriton wakei*. *Zootaxa* **3795:** 61–70.

Miller MA, Pfeiffer W, Schwartz T. 2010. Creating the CIPRES Science Gateway for inference of large phylogenetic trees. *Proceedings of the Gateway Computing Environments Workshop (GCE)*: 1–8.

Milne I, Linder D, Bayer M, Husmeier D, McGuire G, Marshall DF, Wright F. 2009. TOPALi v2: a rich graphical interface for evolutionary analyses of multiple alignments on HPC clusters and multi-core desktops. *Bioinformatics* **25:** 126–127.

Myers CW. 1969. The ecological geography of cloud forests in Panama. *American Museum Novitates* **2396:** 1–52.

Ornelas JF, Ruiz-Sánchez E, Sosa V. 2010. Phylogeography of *Podocarpus matudae* (Podocarpaceae): pre-Quaternary relicts in northern Mesoamerican cloud forests. *Journal of Biogeography* **37:** 2384–2396.

Ornelas JF, Sosa V, Soltis DE, Daza JM, Gonzalez C, Soltis PS, Gutierrez-Rodriguez C, de los Monteros AE, Castoe TA, Bell C, Ruiz-Sanchez E. 2013. Comparative phylogeographic analyses illustrate the complex evolutionary history of threatened cloud forests of northern Mesoamerica. *PLoS One* **8:** e56283.

Parra-Olea G. 2003. Phylogenetic relationships of the genus *Chiropterotriton* (Caudata: Plethodontidae) based on 16S ribosomal mtDNA. *Canadian Journal of Zoology* **81:** 2048–2060.

Rannala B, Yang Z. 2013. Improved reversible jump algorithms for Bayesian species delimitation. *Genetics* **194:** 245–253.

Ree RH, Moore BR, Webb CO, Donoghue MJ. 2005. A likelihood framework for inferring the evolution of geographic range on phylogenetic trees. *Evolution* **59:** 2299–2311.

Ree RH, Smith SA. 2008a. Lagrange: software for likelihood analysis of geographic range evolution. Version 2. Available at: http://code.google.com/p/lagrange/.

Ree RH, Smith SA. 2008b. Maximum likelihood inference of geographic range evolution by dispersal, extinction, and cladogenesis. *Systematic Biology* **57:** 4–14.

Ronquist F, Teslenko M, van der Mark P, Ayres DL, Darling A, Hohna S, Larget B, Liu L, Suchard MA, Huelsenbeck JP. 2012. MrBayes 3.2: efficient Bayesian phylogenetic inference and model choice across a large model space. *Systematic Biology* **61:** 539–542.

Rovito SM, Wake DB, Papenfuss TJ, Parra-Olea G, Muñoz-Alonso A, Vásquez-Almazán CR. 2012. Species formation and geographical range evolution in a genus of Central American cloud forest salamanders (*Dendrotriton*). *Journal of Biogeography* **39:** 1251–1265.

Ruiz-Sánchez E, Ornelas JF. 2014. Phylogeography of *Liquidambar styraciflua* (Altingiaceae) in Mesoamerica: survivors of a Neogene widespread temperate forest (or cloud forest) in North America? *Ecology and Evolution* **4:** 311–328.

Schuchert C. 1935. *Historical geology of the Antillean-Caribbean region*. New York: John Wiley and Sons.

Stadtmüller T. 1987. *Cloud forests in the humid tropics*. Tokyo: The United Nations University.

Stamatakis A. 2006. RAxML-VI-HPC: maximum likelihood-based phylogenetic analyses with thousands of taxa and mixed models. *Bioinformatics* **22:** 2688–2690.

Stephens M, Smith NJ, Donnelly P. 2001. A new statistical method for haplotype reconstruction from population data. *American Journal of Human Genetics* **68:** 978–989.

Swofford DL. 2003. *PAUP*. Phylogenetic analysis using parsimony (*and other methods), version 4.0*. Sunderland: Sinauer Associates.

Tavaré S. 1986. Some probabilistic and statistical problems in the analysis of DNA sequences. *Lectures on Mathematics in the Life Sciences* **17:** 57–86.

Townsend JH, Butler JM, Wilson LD, Austin JD. 2010. A distinctive new species of moss salamander (Caudata: Plethodontidae: *Nototriton*) from an imperiled Honduran endemism hotspot. *Zootaxa* **2434:** 1–16.

Townsend JH, Medina-Flores M, Murillo JL, Austin JD. 2011. Cryptic diversity in the Chortís Highland moss salamanders (Caudata: Plethodontidae: *Nototriton*) revealed using mtDNA barcodes and phylogenetics, with a new species from eastern Honduras. *Systematics and Biodiversity* **9:** 275–287.

Vásquez-Almazán CR, Rovito SM, Good DA, Wake DB. 2009. A new species of *Cryptotriton* (Caudata: Plethodontidae) from eastern Guatemala. *Copeia* **2009:** 313–319.

Wake DB. 1987. Adaptive radiation of salamanders in Middle American cloud forests. *Annals of the Missouri Botanical Garden* **74:** 242–264.

Wake DB, Elias P. 1983. New genera and a new species of Central American salamanders, with a review of the tropical genera (Amphibia, Caudata, Plethodontidae). *Contributions in Science (Los Angeles)* **345:** 1–19.

Wake DB, Lynch JF. 1976. The distribution, ecology and evolutionary history of plethodontid salamanders in tropical America. *Natural History Museum of Los Angeles County Science Bulletin* **25:** 1–65.

Wake DB, Rovito SM, Maisano JA, Hanken J. 2012. Taxonomic status of the enigmatic salamander *Cryptotriton adelos* (Amphibia: Plethodontidae), from northern Oaxaca, Mexico, with observations on its skull and postcranial skeleton. *Zootaxa* **3579:** 67–70.

Wiens JJ, Parra-Olea G, García-París M, Wake DB. 2007. Phylogenetic history underlies elevational biodiversity patterns in tropical salamanders. *Proceedings of the Royal Society Biological Sciences Series B* **274:** 919–928.

Yang Z, Rannala B. 2010. Bayesian species delimitation using multilocus sequence data. *Proceedings of the National Academy of Sciences of the United States of America* **107:** 9264–9269.

APPENDIX

Specimens examined for morphological analysis.

Cryptotriton alvarezdeltoroi: Mexico: Chiapas: IBH 29568, 1.7 km N (by rd) of highway from Tapalapa to Pantepec on road to Maxono; MVZ 158942, 21.5 km N Jitotol on Mexico Highway 195; MVZ 201396, Puerto del Viento, 13 km NW Pueblo Nuevo Solistahuacán. *Cryptotriton monzoni*: Guatemala: Zacapa: MVZ 265529–265530: 5.2 km SE (by road) of center of La Unión. *Cryptotriton nasalis*: Guatemala: Izabal: UTA A-50002, Cerro Pozo del Agua, Sierra de Caral; Honduras: Cortés: MVZ 128273–128274, Sierra de Omoa, 10 km WSW (by air) San Pedro Sula; MVZ 263810, El Cusuco; MVZ 263836: mountains west of San Pedro Sula. *Cryptotriton necopinus*: Honduras: Francisco Morazán: MVZ 269392, Montaña de Yoro. *Cryptotriton sierraminensis*: Guatemala: Zacapa: MVZ150882–150883, 150885–150887, 150889–150891, 150893–150898, 11 km N Santa Cruz, Volcán de Los Monos; MVZ 160898, 160900–160904, 160906–160912, 10.5 km N of CA-9 km 126 at Santa Cruz, Sierra de Las Minas; MVZ 150901–150912, 150915–150917, 150919, 150921–150922, 167992, 15 km NNE of Rio Hondo, Finca Planada. *Cryptotriton veraepacis*: Guatemala: Baja Verapaz: MVZ 167773, 167783–167786, 167967–167972, 167991, 167993–167996, 215913, 6.5 mi ESE Purulhá; MVZ 172702, 2.5 mi S Purulhá. *Cryptotriton xucaneborum*: Guatemala: Alta Verapaz: MVZ 263575, 3.8 km (by road) south of Finca El Volcán, Senahú; MVZ 269514–517: Chelemhá Cloud Forest Reserve. *Cryptotriton sp*.: Guatemala: Alta Verapaz: MVZ 265639, 1.9 km S (by air) of Bethel, 5.0 km N (by rd) of Sacristal-San Pedro Carchá road.

SUPPORTING INFORMATION

Additional Supporting Information may be found in the online version of this article at the publisher's web-site:

Figure S1. Phylogenetic tree from maximum likelihood analysis of all loci concatenated into a single data matrix. Numbers above branches are bootstrap support values from ML analysis, and numbers below branches are posterior probabilities from Bayesian analysis. Bootstraps below 50 and posterior probabilities below 0.5 are not shown.
Figure S2. Phylogenetic tree from maximum likelihood analysis of nuclear loci concatenated into a single data matrix. Numbers above branches are bootstrap support values from ML analysis, and numbers below branches are posterior probabilities from Bayesian analysis. Bootstraps below 50 and posterior probabilities below 0.5 are not shown.
Table S1. Voucher information for samples used in phylogenetic analysis. Institutional abbreviations: MVZ, Museum of Vertebrate Zoology, University of California, Berkeley; USAC, Museo de Historia Natural, Universidad de San Carlos, Guatemala.
Table S2. Primers, PCR conditions, and alignment lengths for gene fragments used in phylogenetic analyses.
Table S3. GenBank numbers for sequences used in phylogenetic analyses.